
New Developments in Rock Fall Hazard Assessment and Zoning: An Application of the Cadanav Methodology

355

Jacopo M Abbruzzese and Vincent Labiouse

Abstract

Rock fall hazard assessment and zoning are very important for an appropriate land use planning in mountainous areas. However, they are complex topics, and current methodologies adopted for producing zoning maps do not provide satisfactory results, due to assumptions and uncertainties involved in hazard assessment. This paper presents an application of the Cadanav methodology, which attempts at reducing hypotheses and related uncertainties particularly affecting the use of rock fall modelling results and the techniques for combining energy and frequency. This procedure allows for a quantitative evaluation of rock fall hazards based on the combination of relevant parameters also determined in quantitative terms. The hazard is obtained at any point of the slope by means of a new tool defined as “hazard curve”. Aimed to hazard degree assessment and zoning at the local scale, the Cadanav methodology is presented with reference to a case study set in the Canton of Valais (Switzerland). Different scenarios in terms of rock fall frequency are considered, to illustrate how this procedure can also describe the way hazard evolves along the slope, if a change in the probability of failure occurs.

Keywords

Rock fall • Trajectory modelling • Hazard assessment • Hazard zoning • Land use planning

355.1 Introduction

Landslides threaten many communities located in mountainous areas all over the world, and cause important economic losses every year. Rock falls are among these phenomena, and represent one of the major causes of fatalities associated to landslides, due to the high energy and mobility of the blocks. These processes must necessarily be taken into account in urban planning, in order to guarantee safety for human lives, properties and activities in all the areas which could be potentially affected.

According to the most recent definitions widely accepted at the international level (Fell et al. 2005, 2008; MR 2010), landslide hazard has to be characterised based on the frequency (or probability) of failure of the process, its likelihood of impacting a given point of the slope and its intensity. For rock fall problems, this means determining how often blocks detach from potentially unstable cliffs, what probability the blocks have of reaching a specific location on the slope surface, and the kinetic energy characterising their trajectories.

Several methodologies are currently available for coping with rock fall problems (Desvarreux 2007; Rouiller et al. 1998; Jaboyedoff et al. 2005; Mölk et al. 2008; InterregIIc 2001; Mazzoccola and Sciesa 2000; Crosta and Agliardi 2003; Chau et al. 2004; Lan et al. 2007), even though the assumptions they are based on do not allow to combine all the parameters required for hazard assessment in a rigorous manner. Hypotheses and related uncertainties affect every

J.M. Abbruzzese (✉) · V. Labiouse
École Polytechnique Fédérale de Lausanne (EPFL), School of
Architecture, Civil and Environmental Engineering (ENAC),
Laboratory for Rock Mechanics (LMR), Lausanne, Switzerland
e-mail: jacopo.abbruzzese@gmail.com

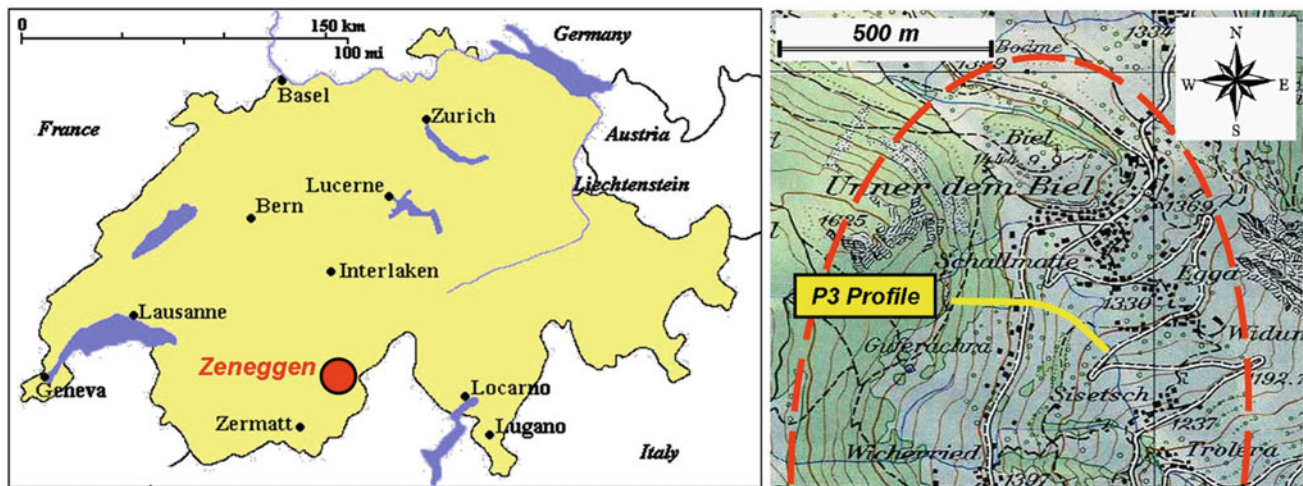


Fig. 355.1 Left: location of Zeneggen, Valais, Switzerland (source <http://www.safaritheglobe.com>). Right: map of the study area—within the red dashed line (source Swisstopo)

aspect of the hazard zoning process, and may involve, among others:

- the evaluation of the failure frequency, which different methodologies may consider either qualitatively (Rouiller et al. 1998; Mazzocola and Sciesa 2000) or quantitatively (Jaboyedoff et al. 2005; Chau et al. 2004), or even not at all, in some cases (Desvarreux 2007; Lan et al. 2007);
- the use of the raw trajectory modelling results, for what concerns e.g. the number of trajectories to be run and how to treat possible outliers (Abbruzzese et al. 2009);
- the definition of rock fall energy values at a given point of the slope, as well as the methods for combining the necessary parameters (energy and probability of occurrence), possibly according to intensity-frequency diagrams — if planned (Raetzo et al. 2002; Altimir et al. 2001).

In this context, the Cadanav methodology focuses on the second and third issues, and attempts at reducing uncertainties affecting the use of trajectory modelling results and the techniques for combining rock fall frequency and energy. With the help of an application to a real site, the following Sections illustrate how the relevant parameters are determined and combined for performing hazard zoning along a 2D slope profile, starting from the results of 2D trajectory simulations.

355.2 Study Area and Rock Fall Simulation Set-Up

The new Cadanav methodology was applied at the site of Zeneggen, located in the Canton of Valais in Switzerland (Fig. 355.1). The cliffs in this area are mainly composed of hard rocks of gneiss and mica, and are characterised by five main discontinuity sets.

The profile selected for performing hazard zoning is identified as P3 (Fig. 355.1). As shown in Fig. 355.3, the upper part of the slope is covered by scree deposits and moraines, while more downhill a grassy soft soil area is found. According to the site observations, events which may occur in this area are characterised by block volumes ranging from 1 to 5 m³.

For this application, rock fall simulations were performed considering the maximum block volume of 5 m³. The trajectories were computed by the geological firm Géoval (Canton of Valais) with the Rockfall 6.0 code (Spang and Krauter 2001), and 10,000 trajectories were run. Based on the field investigations (and on the capabilities of the rock fall code), the blocks were assumed as cylindrical boulders with a length of 1.4 m, whose radius equals the 75 % of the block length. An initial velocity of 1 m/s was assigned for simulating a translational failure mechanism.

355.3 Hazard Analysis According to the Cadanav Methodology

The Cadanav methodology (Abbruzzese 2011; Abbruzzese and Labiouse 2013) defines the hazard as:

$$\lambda(E, x) = \lambda_f \cdot P_r(E, x) \cdot d \quad (355.1)$$

where $\lambda(E, x)$ expresses the hazard as a mean annual number of blocks hitting a given point of the slope (i.e. abscissa x) with an energy higher than E , λ_f is the rock fall frequency of failure, $P_r(E, x)$ is the probability of a block hitting a point of the slope x with energy higher than E (frequency of reach), and d is a characteristic block size (e.g. maximum dimension of the block, or equivalent diameter).

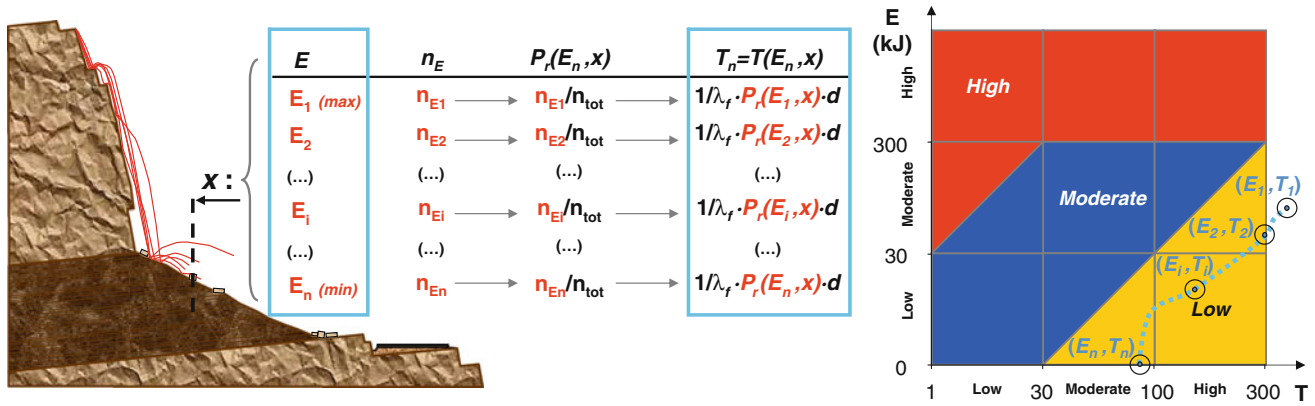


Fig. 355.2 Scheme of computation of the frequency of reach $P_r(E, x)$ and return period T , and use of the hazard curve in combination with the Swiss intensity frequency diagram

For 2D problems involving linear cliffs (Abbruzzese et al. 2009; Hantz 2011; Abbruzzese and Labiouse 2013) like the one presented here, the frequency of failure is given by the number of blocks detaching from the cliff during a given observation time, per linear metre of cliff. It can be determined from historical data series about past events in the study area, and/or by combining these data with a detailed geomechanical characterisation of the cliff. For the purpose of this application, however, the rock fall frequency was not rigorously determined this way, but a high value was simply assumed, equal to 2 blocks falling on average every 3 years per linear metre of cliff, i.e. $\lambda_f = 0.67 \text{ blocks} \cdot \text{year}^{-1} \cdot \text{m}^{-1}$ (i.e. mean failure time t_f of 1.5 years).

The frequency of reach $P_r(E, x)$ at a given abscissa x of the 2D profile is computed from the cumulative energy distribution at that abscissa (Fig. 355.2). In order to do this, all the energy values E obtained at x from the rock fall

simulations were at first ordered. Associated with each ordered energy value, the number of blocks n_E crossing that location with an energy higher than E was subsequently determined. The probability $P_r(E, x)$ was then calculated by normalising each number of blocks n_E obtained by the total number of trajectories computed from the source point.

Regarding the diameter of the block d , this parameter was set equal to the maximum block dimension, i.e. the block length, and it is therefore equal to 1.4 m.

In this study, the Cadanav methodology was applied according to the Swiss Guidelines for landslide hazard zoning (Raetzo et al. 2002), which implies the use of the intensity-frequency diagram shown in Fig. 355.2. In this diagram, the information on rock fall frequency of occurrence — i.e. the frequency of failure λ_f multiplied by the frequency of reach $P_r(E, x)$ — is expressed in terms of return period. Therefore, Eq. (355.1) must also be expressed in

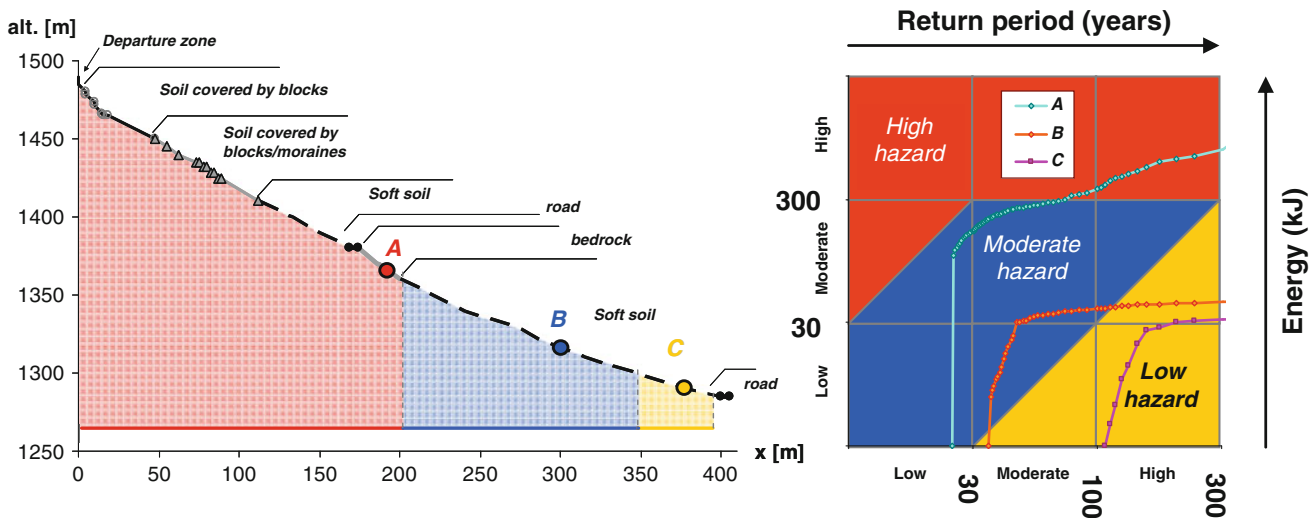


Fig. 355.3 Left: Hazard zoning along the P3 profile at Zeneggen (Valais, Switzerland), for a 5 m^3 block volume and a failure frequency of $\lambda_f = 0.67 \text{ blocks year}^{-1} \text{ m}^{-1}$. Right: Hazard curves at the abscissas $x = 180 \text{ m}$ (Point A), $x = 300 \text{ m}$ (Point B) and $x = 375 \text{ m}$ (Point C)

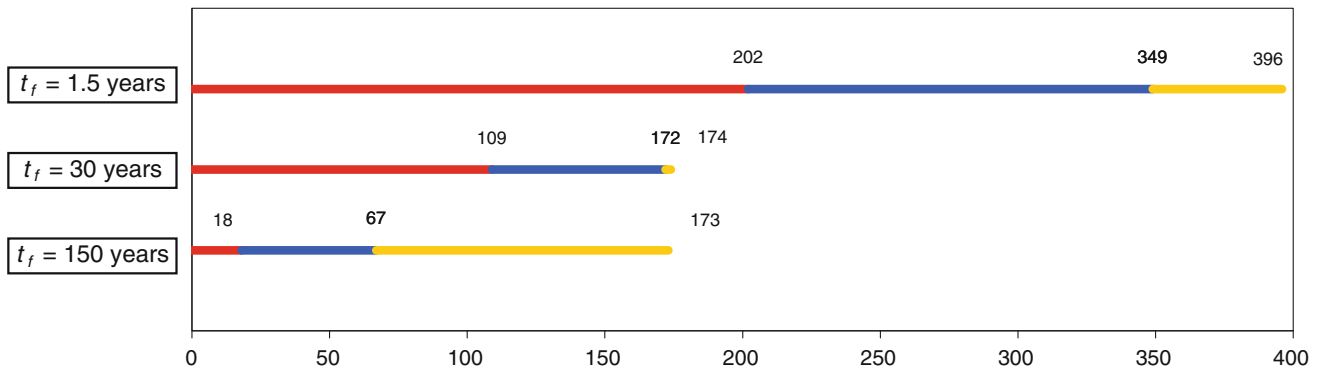


Fig. 355.4 Influence of a change in the rock fall mean failure time t_f on hazard zoning

terms of return period $T(E, x)$, i.e. inverse of the mean annual frequency given by $\lambda(E, x)$, as follows:

$$T(E, x) = \frac{1}{\lambda(E, x)} = \frac{1}{\lambda_f \cdot P_r(E, x) \cdot d} \quad (355.2)$$

By applying Eq. (355.2) for each value of frequency of reach $P_r(E, x)$ computed at a given point of the slope x , that abscissa is then characterised by as many return period values $T(E, x)$. Considering that each $T(E, x)$ value is associated with the corresponding energy value E , a set of energy-return period couples $E-T(E, x)$ can be defined, which represent all the possible hazardous conditions potentially affecting the abscissa x .

As a whole, these couples can be seen as a curve, called “hazard curve”, which can finally be superimposed to an intensity-frequency matrix diagram, like the Swiss one (Fig. 355.2). The hazard at x can then be qualified as e.g. high, moderate or low, depending on which area(s) of the diagram the couples are located in. In particular:

- if all the energy-return period couples are located in an area of the diagram characterised by the same hazard degree (e.g. low hazard), the abscissa x is assigned that degree of hazard (e.g. low);
- if the couples are in different areas, i.e. they represent more than one degree of hazard, x is assigned the most unfavourable among them.

The application of Eq. (355.2) and the use of the hazard curves in combination with the Swiss diagram were repeated at each abscissa of the profile, which allowed to completely characterise the hazard all along the slope. Figure 355.3 shows the results obtained for the profile selected at Zeneggen, for the frequency of failure scenario assumed, i.e. $\lambda_f = 0.67$ blocks·year⁻¹·m⁻¹. Hazard curves are illustrated for three points A, B and C, located at $x = 180$ m, $x = 300$ m and $x = 375$ m, respectively. The curve corresponding to Point A intersects both the moderate and the high hazard areas of the Swiss diagram; according to the criterion reported just above, this abscissa must be thus characterised by a high

hazard degree. Similarly, the curve referred to Point B intersects the moderate and low hazard areas, i.e. the hazard degree at this abscissa is moderate. Finally, at Point C all the energy-return period couples are in the low hazard area of the diagram, so the hazard degree is qualified as low. As one could expect, the hazard degree decreases when moving from the rock fall source area down slope (from Point A to C), and the hazard curves allow to effectively describe and visualise this variability in space.

Furthermore, as in the Cadnav methodology the frequency of failure must be introduced in quantitative terms, also the evolution of hazard in time can be well accounted for. Figure 355.4 illustrates the effects on zoning when a change in the rock fall failure frequency occurs (due for instance to changes in triggering factors). Three failure frequency scenarios were considered, for decreasing values of λ_f , i.e. $\lambda_f = 0.67, 0.033$ and $6.7 \cdot 10^{-3}$ blocks·year⁻¹·m⁻¹ (corresponding to mean failure times t_f of 1.5, 30 and 150 years, respectively). It was here assumed that the related event and block volumes do not change, though.

It can be observed that a decrease in the number of events per year clearly produces a lower degree of hazard all along the slope, accordingly described by the fact that the boundaries of each hazard zone move up slope.

355.4 Concluding Remarks

The new Cadnav methodology introduces improvements to quantitative rock fall hazard assessment at the local scale, by reducing assumptions and uncertainties affecting the use of trajectory modelling results and the techniques for combining energy and rock fall frequency of occurrence. The procedure is based on a quantitative definition of energy, frequency of failure and frequency of reach of the blocks (the latter being obtained from rock fall trajectory modelling), and evaluates the hazard by means of “hazard curves”, built at any point of the slope. These curves are constituted by rock fall energy-return period couples, which represent all

the possible hazardous conditions at the location considered. In the application presented, the hazard degree was assessed by superimposing the curves to an intensity-frequency diagram, in order to determine which hazardous condition prevails at any point of interest of the 2D profile selected. It was shown that, together with a rigorous and detailed assessment and zoning of rock fall hazards, the hazard curves constitute a useful tool for visualising and understanding the evolution of hazard in space (all along the slope) and time (at a specific location, if e.g. failure conditions and related rock fall scenarios change).

Acknowledgments The authors would like to thank the European Commission for supporting the PhD research project within which this work was performed. The project was carried out as a part of the Marie Curie Research Training Network “Mountain Risks: from prediction to management and governance”, in the 6th Framework Programme of the European Commission. They would also like to thank the authorities of the Canton of Valais for permitting the publication of the results concerning the study area, and the bureau Géoval for performing the rock fall trajectory simulations.

References

- Abbruzzese JM (2011) Improved methodology for rock fall hazard zoning at the local scale. PhD Thesis, Rock Mechanics Laboratory of the Ecole Polytechnique Fédérale de Lausanne
- Abbruzzese JM, Labiouse V (2013) New Cadnav methodology for quantitative rock fall hazard assessment and zoning at the local scale. *Landslides*. doi:10.1007/s10346-013-0411-7
- Abbruzzese JM, Sauthier C, Labiouse V (2009) Considerations on Swiss methodologies for rock fall hazard mapping based on trajectory modelling. *Nat Hazards Earth Syst Sci* 9:1095–1109
- Altimir J, Copons R, Amigó J, Corominas J, Torredadella J, Vilaplana JM (2001) Zonificació del territori segons el grau de perillositat d’esllavissades al Principat d’Andorra. In: *La Gestió dels Riscos Naturals, 1^{es} Jornades del CRECIT (Centre de Recerca en Ciències de la Terra)*, pp 119–132
- Chau KT, Sze YL, Fung MK, Wong WY, Fong EL, Chan LCP (2004) Landslide hazard analysis for Hong Kong using landslide inventory and GIS. *Comput Geosci* 30:429–443
- Crosta GB, Agliardi F (2003) A methodology for physically based rockfall hazard assessment. *Nat Hazards Earth Syst Sci* 3:407–422
- Desvarreux P (2007) Problèmes posés par le zonage, Lecture notes from the course « Université Européenne d’été 2007: éboulements, chutes de blocs – rôle de la forêt », Courmayeur, Sept 2007
- Fell R, Corominas J, Bonnard C, Cascini L, Leroi E, Savage WZ; on behalf of the JTC-1 Joint Technical Committee on Landslides and Engineered Slopes (2008) Guidelines for landslide susceptibility, hazard and risk zoning for land use planning. *Eng Geol* 102:85–98
- Fell R, Ho KKS, Lacasse S, Leroi E (2005) A framework for landslide risk assessment and management. In: Hungr O, Fell R, Couture R, Eberhardt E (eds) *Landslide risk management*. Taylor & Francis Group, London, pp 3–25
- Hantz D (2011) Quantitative assessment of diffuse rock fall hazard along a cliff foot. *Nat Hazards Earth Syst Sci* 11:1303–1309
- Interreg IIC (2001) Prévention des mouvements de versants et des instabilités de falaises: confrontation des méthodes d’étude d’éboulements rocheux dans l’arc Alpin, Interreg Communauté Européenne
- Jaboyedoff M, Dutt JP, Labiouse V (2005) An attempt to refine rockfall hazard zoning based on the kinetic energy, frequency and fragmentation degree. *Nat Hazards Earth Syst Sci* 5:621–632
- Lan H, Derek MC, Lim HC (2007) RockFall Analyst: a GIS extension for three-dimensional and spatially distributed rockfall hazard modeling. *Comput Geosci* 33:262–279
- Mazzoccola D, Sciesa E (2000) Implementation and comparison of different methods for rockfall hazard assessment in the Italian Alps. In: *Landslides in theory, research and practice, Proceedings of the 8th international symposium on landslides*, vol 2. Thomas Telford Ltd., London, pp 1035–1040
- Mölk M, Poisel R, Weibold J, Angerer H (2008) Rockfall rating systems: is there a comprehensive method for hazard zoning in populated areas? In: *Proceedings of the 11th INTERPRAEVENT 2008 congress*, vol 2, pp 26–30
- MR (Mountain Risks Research Training Network), Glossary (2010) http://www.unicaen.fr/mountainrisks/spip/spip.php?page=presentation_article&id_article=51#1. Accessed 15 Sept 2010
- Raetzo H, Lateltin O, Bollinger D, Tripet JP (2002) Hazard assessment in Switzerland—codes of practice for mass movements. *Bull Eng Geol Environ* 61:263–268
- Rouiller J-D, Jaboyedoff M, Marro C, Phillipossian F, Mamin M (1998) *Pentes instables dans le Pennique valaisan, Rapport final PNR 31*. VDF, Zürich
- Spang RM, Krauter E (2001) Rockfall simulation—a state of the art tool for risk assessment and dimensioning of rockfall barriers. In: Kühne M et al. (eds) *International conference on landslides—causes, impacts and countermeasures*, pp 607–613